Biomedicine & Pharmacotherapy 165 (2023) 115214

Contents lists available at ScienceDirect

Biomedicine & Pharmacotherapy

journal homepage: www.elsevier.com/locate/biopha

Short communication

In-vivo anti-diabetic and anti-hyperlipidemic effects of natural metabolites from resin of *Commiphora mukul* and their *in-silico* to *in-vitro* target fishing

Waseem Ul Islam [a], Faizullah Khan [b], Muhammad Waqas [b], Saeed Ullah [b], Sobia Ahsan Halim [b], Najeeb Ur Rehman [b], Hanif Khan [c], Mohamed H. Mahmoud [d], Gaber El-Saber Batiha [e], Ajmal Khan [b,*], Ahmed Al-Harrasi [b,*]

[a] Department of Pharmacy, University of Swabi, Khyber Pakhtunkhwa, Pakistan
[b] Natural and Medical Sciences Research Center, University of Nizwa, P.O. Box 33, Birkat Al Mauz, Nizwa 616, Sultanate of Oman
[c] Department of Cell Systems and Anatomy, School of Medicine, University of Texas Health Science Center at San Antonio, TX 78229, USA
[d] Department of Biochemistry, College of Science, King Saud University, Kingdom of Saudi Arabia
[e] Department of Pharmacology and Therapeutics, Faculty of Veterinary Medicine, Damanhour University, Damanhour 22511, AlBeheira, Egypt

ARTICLE INFO

Keywords:
Antidiabetic
Antihyperlipdimic
Myrrhanone-B
Myrrhanol-B
α-glucosidase
Docking

ABSTRACT

Diabetes mellitus is a rapidly spreading global metabolic disorder that has serious social, health, and economic consequences. Herein, we have evaluated *in vivo* antidiabetic and antihyperlipidemic effects of myrrhanone-B and myrrhanol-B (isolated from *Commiphora mukul* Hook). We observed that treatment with myrrhanone-B and myrrhanol-B at a dose of 5 and 10 mg/kg body weight for 21 days significantly improved body weight loss, water consumption, and the concentration of blood glucose level (BGL) in alloxan (120 mg/kg) induced diabetic mice, which indicates that the compounds possess strong anti-diabetic activities. In the biochemical analysis, these compounds improved an abnormal level of total cholesterol (TC), triacylglycerol (TG), and low-density lipoprotein cholesterol (LDL-C) to a normal level and increased the high-density lipoprotein cholesterol level (HDLC). Later, drug target of compounds was predicted through *in-silico* docking which shows that these compounds nicely fit in the active site of α-glucosidase enzyme and mediates excellent interactions with the catalytic residues, Asp214 and Asp349. The *in-silico* results were confirmed by *in-vitro* testing of myrrhanone-B and myrrhanol-B against α-glucosidase where both the compounds exhibited excellent inhibitory potency with IC_{50} values of 19.50 ± 0.71, and 16.11 ± 0.69 μM, respectively. Furthermore, mechanistic study was conducted to observe their binding mechanism, which reflect that myrrhanol-B has mixed type of inhibition (ki = 12.33 ± 0.030 μM), while myrrhanone-B demonstrates competitive type of inhibition (ki =14.53 ± 0.040 μM).

1. Introduction

The burden of diabetes extends beyond the sheer number of people it affects to its effects on the economy and healthcare systems. Non-insulin dependent diabetes mellitus (NIDDM) influences majority of diabetic individuals. A key aspect of the pathophysiology of human NIDDM is the presence of pancreatic cell abnormalities as well as resistance to the biological activities of insulin in the liver and peripheral organs [1,2]. Diabetes is linked to an increased risk of amputations, renal disease, stroke, cardiovascular disease, and blindness [3]. Diabetes management calls for ongoing observation, lifestyle adjustments, and frequent medication. Health care systems and people are heavily burdened by the cost of treating diabetes, particularly in low and middle income nations where resources are insufficient [4]. Diabetes is influenced by both genetic and environmental factors, with variable prevalence rates in different ethnic groups and populations [5]. According to estimates, there were 463 million persons with diabetes worldwide in 2019. By 2030 and 2045, that number is expected to rise to 578 million (10.2%)

Abbreviations: DM, Diabetes mellitus; IP, Intraperitoneal; ALP, Alanine pyruvate; ANOVA, One-way analysis of variance; ATP, Adenine triphosphate; BGL, Blood glucose level; GM, Gram; IDDM, Insulin-dependent diabetes mellitus; NIDDM, Non-Insulin dependent diabetes mellitus; IGT, Impaired glucose tolerance; LDL, Low-density lipoprotein; HDL, High-density lipoprotein; LFTs, Liver function tests; TC, Total cholesterol; SGOT, Serum glutamic-oxaloacetic transaminase; ADA, American diabetic association; SGPT, Serum glutamic pyruvic transaminase.

* Corresponding authors.
E-mail addresses: ajmalkhan@unizwa.edu.om (A. Khan), aharrasi@unizwa.edu.om (A. Al-Harrasi).

https://doi.org/10.1016/j.biopha.2023.115214
Received 5 June 2023; Received in revised form 12 July 2023; Accepted 21 July 2023
Available online 27 July 2023

and 700 million (10.9%), respectively. Urban areas (10.8%) have a greater incidence than rural areas (7.2%), and high-income countries (10.4%) have a higher prevalence than low income countries (4%) [6]. Additionally, obese and physically inactive individuals have a history of the disease in their families, and consumption of unhealthy diets impose higher risk of diabetes [7]. Reducing the burden of diabetes requires prevention and early detection. Type 2 diabetes can be prevented or delayed with lifestyle changes such keeping a healthy weight, engaging in regular exercise, and eating a balanced diet [8]. For an early diagnosis and effective treatment of the condition, screening for diabetes and its consequences is also crucial. However, there is still a big problem with access to diabetes care, especially in low- and middle-income nations [9]. As a result, scientists are investigating a variety of strategies, such as the use of natural products, gene therapy, and stem cell therapy [9]. The search for novel chemical compounds with particular biological properties that can control glucose homeostasis and enhance insulin sensitivity is another step in the development of new diabetic medications [10].

Natural substances have drawn a lot of attention in drug discovery in recent years due to their variety of biological and pharmacological features [11–14]. It is well recognized that substances derived from natural sources have anti-inflammatory, anti-cancer, anti-bacterial, anti-fungal, and antiviral properties [15]. These substances may be used in the creation of novel diabetic medications because they have been documented to have hypoglycemic activity in the context of diabetes [16].

The genus Commiphora, which includes about 190 species, is found in southern Arabia, India, and Sri Lanka. One of these species is *Commiphora mukul* Hook. ex-Stocks (Burseraceae) [17,18]. For more than 2000 years, the Oleo-gum resin of *C. mukul* (gugulipid), produced by the plant's stem, has been used to cure arthritis, inflammation, and to enhance the hepatic antioxidant defense system. It has been used as an anti-inflammatory, anti-obesity, anti-coagulant, anti-bacterial, and anti-atherosclerosis agent in traditional medicines of India and many Arabian countries. It also exhibits a wide range of pharmacological effects, including cytotoxicity, lipid disorders, anesthetic, and anti-diabetics [17,19,20]. It has been suggested for a number of human diseases, such as liver [21–23]. *C. opobalsamum* extract possesses hepatoprotective, hypotensive, and anti-ulcerogenic properties in rats in traditional Arabian medicine [24–26]. The resin of *C. mukul* has previously been subjected to phytochemical analysis, which resulted in the isolation of a number of lignans, sterols, triterpenes, oligosaccharides, diterpenoids, and sesquiterpenes [17,27]. The resin of *C. mukul* has previously been subjected to phytochemical analysis, which resulted in the isolation of a number of lignans, sterols, triterpenes, oligosaccharides, diterpenoids, and sesquiterpenes [17], both analgesic and anti-inflammatory effects [19]. Additionally, some substances have been used as painkillers and have shown to have the ability to suppress the generation of nitric oxide [19,28]. The aim of our current research work is to develop novel molecules that are biologically active specifically against diabetes. In this paper, we report the antidiabetic and anti-hyperglycemic potential of two natural compounds, myrrhanone-B, and myrrhanol-B in the *in vivo* studies. Furthermore, the molecular target of these compounds was predicted *in-silico* method and confirmed by *in-vitro* studies.

2. Material and method

2.1. Chemicals

The chemicals utilized in this trial were alloxan (Sigma-Aldrich), glibenclamide (Sanofi Aventis Pharma (Pvt.) Ltd., Pakistan), and glucose measurement kits (ACCU CHECK). The various organic solvents and chemicals used in the experiment were bought from local Merck, Germany, sources. Normal saline (Utsoka Pharma (Pvt) Ltd., Pakistan), biochemical reagents for lipid profile, LFTs Kits (Human, Germany), and RFTs kit (Bioneed Germany diagnosis) were also used in this investigation.

2.2. Extraction and isolation of the compounds

C. mukul (2.0 kg) resin was obtained from local market of Nizwa, Oman and identified by the plant taxonomist at the Department of Biological Sciences and Chemistry, University of Nizwa, Oman. A voucher specimen (CMS-05/2018) was deposited in the herbarium of the Natural and Medical Sciences Research Center (NMSRC), University of Nizwa, Oman. The powder resin (1.2 Kg) was extracted with methanol (3.0 L) through sonicator at room temperature for one day (3 times). The methanol extract was dried by evaporating solvent under reduced pressure to obtain the methanol extract (840 g), which was further fractionated into *n*-hexane (266 g), dichloromethane (120 gm), ethyl acetate (210 g), *n*-butanol (115 g), and aqueous (90 g) following the published protocol [29]. The *n*-hexane (220 g) fraction was subjected to silica gel column chromatography (70–230 mesh; Merck), using the 10–20% *n*-hexane/ethyl acetate solvent system as an eluent to give two compounds; myrrhanone-B (240 mg) and myrrhanol-B (550 mg) [17, 29].

2.3. Animal

For the *in-vivo* study, Swiss Albino mice that were 3–4 weeks old and weighed 20–30 gm were used. These animals were purchased from the National Institute of Health (NIH) in Islamabad, Pakistan, and kept in sanitary boxes with appropriate laboratory equipment. In the animal house, the animals were kept on a 12-hour light/dark cycle at a constant room temperature of 22–25 °C. The departmental animal ethical committee has given its approval to all animal procedures with (DAEC/PHARM/2016/15) University of Swabi, KPK, Pakistan and were carried out in compliance with the 1986 UK Animal Scientific Procedure Act.

2.4. Design of the experiment

Seven groups of the Swiss albino mice were created, each including six mice (n = 6). Group I functioned as the negative control and merely received normal saline only. Group II served as the diabetic control group received no treatment at all, while Group III was treated with simply glibenclamide (0.5 mg/kg), served as the standard. Group IV and V received compound myrrhanol-B at a dose of 5 mg/kg and 10 mg/kg, respectively and Groups VI and VII were administered with myrrhanone-B at a dose of 5 mg/kg and 10 mg/kg, respectively. Compounds were injected intraperitoneally (i.p.) for a total of 21 days, these compounds were administered to the animal once daily at 9:00 a.m. Estimates of body weight and blood sugar levels were made on the first, fourth, seventh, tenth, fifteenth and twenty-first days of treatment.

2.5. Toxicity study

According to the procedure outlined by Irwin, Swiss albino mice weighing between 20 and 30 g were used to test the acute toxicity of myrrhanone-B and myrrhanol-B [30]. For myrrhanone-B and myrrhanol-B, the animals were splitted into six groups (n = 6). Group 1 served as the control and merely received normal saline. While myrrhanone-B and myrrhanol-B were administered to further groups (Groups II through Group VI) at doses of 5, 10, 20, 40, and 50 mg/kg i.p. Weirding, convulsions, aggression, hypersensitivity, salivation, lacrimation, spontaneous activity, ataxia, and catalepsy were only a few of the criteria that each animal was tested for, 30 min prior to injection (baseline), at 0 (immediately following injection), at 30 and 60 min, at 24, 48, and 72 h, and at 1 week following administration. The same kinds of physiological, behavioral, and pharmacological harmful effects were monitored in all of the animals [31].

2.6. Induction of hyperglycemia

A single intraperitoneal (i.p.) injection of alloxan (120 mg/kg) reconstituted with ice-cold normal saline (0.9%) caused hyperglycemia in overnight fasting Swiss albino mice [32]. Blood was drawn from a tail vein puncture after 72 h of alloxan injection and glucose levels were estimated using one-touch Glucometer strips and an ACCU CHECK glucometer. Diabetic mice were chosen for the investigation if their fasting blood glucose levels were greater than 240 mg/dl.

2.7. Estimation of serum lipid and liver physiological profile

After the accomplishment of antidiabetic experiment on the 21st day, all the animals were anesthetized by pentobarbital sodium (35 mg/kg) and euthanized by cervical decapitation using the method described in schedule 1 of the Animal Scientific Procedure Act 1986 and blood samples were collected through cardiac puncture for biochemical parameters studies [33]. Collected blood was centrifuged at 1500 g for 10 min for serum separation. The serum sample was then analyzed by a spectrophotometer (Perkinelmer, Germany) to determine serum SGPT, SGOT and alkaline phosphatase (ALP) using a standard IFCC kinetic Method (Bioneed kit, Germany). Total cholesterol (TC), triglycerides (TGs), low density lipoproteins (LDL), high density lipoprotein (HDL) and serum creatinine were determined by CHOD-PAP and GPO-PAP methods on a UV-Spectrophotometer using a Human kit, Germany [34].

2.8. Statistical analysis

The mean ± S.E.M (standard error mean) was used to represent all the blood glucose, body weight, and biochemical parameter values. Student's t-test was used to compare two groups, and one-way ANOVA followed by Dunnett's posthoc multiple comparison test was used to compare more than two groups. At $p < 0.05$, differences between groups were deemed significant.

2.9. Computational analysis

In order to predict the biological target of our compounds, α-glucosidase enzyme was chosen for docking studies. *Saccharomyces cerevisiae* α-glucosidase enzyme with entry code P38158 (https://alphafold.ebi.ac.uk/entry/P38158) was taken from AlphaFold Protein Structure Database. To add the missing hydrogens, van der Waals, atom types, angle and bond length parameters, and residues chirality, the Molecular Operating Environment version 2022.02 (MOE) [35] embedded tool QuickPrep was utilized. The Amber14:EHT (Amber ff14SB combined with EHT) forcefield was used to refine the protein structure [36,37].

2.10. Refinement of the α-glucosidase homology-based model

Refining a protein model is a crucial step towards achieving a successful protein model prediction. Molecular dynamic simulation-based approaches are known to yield consistent improvement in the refinement of protein models. In the current study, the protein model of α-glucosidase obtained from the AlphaFold server was refined using a long-run molecular dynamic (MD) simulation. The AMBER22 MD engine was used with an implicit solvent approach, and the amino acid-specific forcefield ff19SB [38] was utilized to generate the protein topology and coordinate files. To neutralize the system, monovalent OPC (optimal point charge) ions including Na+ and Cl- were added at a concentration of ~0.1 M. The missing hydrogens of the protein residues were handled using the Leap module of AMBER22, and a truncated octahedral box of OPC water model was added to solvate the system with a 10 Å buffer distance. The long-range electrostatics were calculated using the GPU-based version Particle Mesh Ewald Molecular Dynamics (PMEMD) [39] of AMBER22, with a cutoff distance of 8 Å. The protein was minimized using two algorithms, steepest descent algorithm minimization for 20,000 steps followed by conjugate gradients minimization algorithm for 10,000 steps [40]. The system was gradually heated and optimized for density from 0.1 k to 300 k using a Langevin thermostat [41] in a 400 ps time and 2.0 ps-1 collision frequency. The system was equilibrated in NPT ensemble for 2000 ps at 300 k with an average pressure of 1 atm and a pressure relaxation time of 2 ps before the production run. Hydrogens were subjected to shake with a 2 fs time step [42], and a 1 μs simulation was performed for model refinement in the production run. The production trajectory was written after each 10 ps simulation time.

2.11. Assessment of α-glucosidase refined model

During the MD simulations, the stability of the refined homology model was evaluated using the CPPTRAJ [43] module of AMBER22 by calculating the root mean square deviation (RMSD) based on Cα atoms of the residues. The RMSD was calculated using a 1 μs trajectory, comprising of 100,000 frames for the model, with the first frame of equilibration being used as the reference coordinate. The residual fluctuation of the protein during the MD run was observed with Root mean square fluctuation (RMSF) analysis. The compactness of the protein structure during the production run was evaluated by Radius of gyration (Rg) analysis. The solvent accessible surface area (SASA) was used to assess the surface accessibility of the protein. To analyze the stereochemical quality of the protein structure before and after the MD simulation, the PROCHECK [44] server was used. Ramachandran plots were generated for both the refined simulated model and the model before simulation [45].

2.12. Molecular docking

The 2D-structures of the ligands were generated using ChemDraw software. These structures were then imported into the molecular operating environment (MOE) version 2022.02 [46] compounds database. To convert the 2D structures into 3D shapes, hydrogen atoms were added, and the partial charges were calculated using the MMFF94x force field. The structures were optimized until the root mean square (RMS) gradient reached a value of 0.01 kcal/mol/Å. For the protein preparation, the QuickPrep module of MOE was used before docking. Hydrogen atoms were added to the protein residues, and partial charges were calculated using the AMBER14:EHT force field [46]. The QuickPrep minimization was employed to refine the protein structure up to an RMS gradient of 0.1 kcal/mol/Å. After preparing the protein and ligand files, docking was performed using the Triangle Matcher docking algorithm. Each ligand conformation was scored using the London dG scoring function. The top 30 poses of ligands from the docking placement were further refined using the GBVI/WSA dG algorithm. The final interactions were selected based on their high docking scores and favorable interactions.

2.13. α-Glucosidase inhibitory assay

The α-glucosidase assay was performed using a 50 mM phosphate buffer (pH 6.8). All samples were dissolved in DMSO, an enzyme (2 U/2 ml) 20 μL/well and test samples (0.5 mg/ml) 20 μL/well and 135 μL/well phosphate buffer were loaded into a 96-well plate, followed by 15 min of incubation at 37 °C. Substrate *p*-nitrophenyl-α-D-glucopyranoside (0.7 mM) 25 μL/well was added to the 96-well plate after 15 min of incubation, and readings were measured at 400 nm for 30 min. DMSO 7% was used as a positive control. Percent inhibition was calculated by using the following formula [47]. The kinetics study was carried out by using the same *in vitro* procedure with a slight modification, addition of four different concentrations of substrate, 0.1, 0.2, 0.4, and 0.8 mM and GraFit 7 Erithacus software was used to evaluate kinetics parameters [48].

$$\%Inhibition = \frac{Absorbance\ \ of\ \ control - Absorbance\ \ of\ \ sample}{Absorbance\ \ of\ \ control} \times 100$$

3. Results and discussion

3.1. Isolation and characterization of Myrrhanol-B and Myrrhanone-B

Myrrhanol-B was isolated as colourless oil from the n-hexane fraction of *C. mukul*. The molecular formula ($C_{30}H_{50}O_4$) was determined through the molecular ion peak at *m/z* 497 $[M+Na]^+$ by ESI-MS analysis. The ^1H NMR spectra of Myrrhanol-B displayed signals for seven tertiary methyls, a methane bearing an oxygen function, and three trisubstituted olefins together with a quaternary carbon bearing an oxygen function and a carboxyl carbon. The ^{13}C NMR spectra determined the presence of thirty (30) carbon signals including seven methyls, ten methylenes, six methines, 3 tri-substituted olefins) and seven quaternary carbons having carboxylic acid (δ_c 171.6). Based on the above evidence, the compound was identified as Myrrhanol B, already published in the literature [17, 19]. Myrrhanone-B was obtained as colourless oil having molecular formula ($C_{30}H_{48}O_4$) determined by molecular ion peak at *m/z* 495 $[M+Na]^+$ in the positive ion ESI-MS analysis. The proton and carbon signals in the ^1H NMR and ^{13}C NMR spectra of Myrrhanone-B attributed signals due to seven tertiary methyls, three tri-substituted olefins together with a quaternary carbon bearing an oxygen function, a carboxyl carbon, and a carbonyl carbon. On the basis of spectroscopic techniques, resemblance with reported data [17,19], the compound was named as Myrrhanone B (Fig. 1).

3.2. Acute toxicity test

In the acute toxicity test, giving animals with Myrrhanone B and Myrrhanol B at a dose of 5–50 mg/kg did not cause any appreciable changes in their behavior, as evidenced by the absence of convulsions, respiratory distress, writhing, changes to reflex activity, or mortality. At 50 mg/kg, two out of six mice displayed a little increase in agitation and escape behavior. All the animals were healthy at day one and there were no discernible changes in their behavior or appearance. Up to one week of research, no deaths were noted.

3.3. Antihyperglycemic impact of Myrrhanol-B, and Myrrhanone-B in alloxan induced diabetic mice

Table 1 shows the effects of Myrrhanol-B, Myrrhanone-B, and reference drug, Glibenclamide on serum glucose levels in alloxan-induced diabetic mice. Glibenclamide at a dose of 0.5 mg/kg, i.p significantly lowered fasting blood glucose readings on day 4th, 7th, 10th, 15th and 21st as compared to the diabetic control group. Intraperitoneal (I.P) administration of Myrrhanol-B (dose = 5 and 10 mg/kg) also had a substantial antihyperglycemic impact and markedly decreased blood glucose levels in alloxan-induced diabetic mice starting on the 4th day. The average blood sugar level dropped from 265.2 ± 11–141 ± 22 mg/dl at the highest tested dose, *i.e.*, 10 mg/kg. Likewise, the administration of Myrrhanone-B, at doses of 5 and 10 mg/kg, resulted in a considerable drop in blood glucose levels from 253.8 ± 25–165 ± 10. In contrast to insulin and other synthetic medicines, these naturally isolated substances (myrrhanol-B and myrrhanone-B) showed good antihyperglycemic efficacy and did not show any hypoglycemia effects [49].

3.4. Effects of Myrrhanol-B and Myrrhanone-B on Body Weight in alloxan-induced diabetic mice

Until the study's conclusion (the 21st day of treatment), weight loss in diabetic control (untreated) mice was persistent. Their body weight was significantly reduced throughout this time, dropped by − 11.5%. However, Myrrhanol-B and Myrrhanone-B at dose levels of 5 and 10 mg/kg were able to reverse the alloxan-mediated bodyweight loss, caused considerable improvement in body weight and showed an increase of 8.2% and 6.16% at the highest dose (Table 2). This increase in body weight was compared with Glibenclamide treated mice. The results show that hypoglycemic impact of Myrrhanol-B and Myrrhanone-B is responsible for this reversal of weight loss in the body.

3.5. Effect of Myrrhanol-B, and Myrrhanone-B on body lipid profile in alloxan-induced diabetic mice

The lipid profiles of the experimental and control mice are given in Table 3. As compared to normal control mice, alloxan-induced diabetic control mice showed significantly higher levels of total cholesterol, triglycerides (TG), low-density lipoprotein (LDL) cholesterol, and serum creatinine ($p < 0.01$, $n = 6$ Student's t test). Administration of Myrrhanol-B, and Myrrhanone-B at 5 and 10 mg/kg for 21 days showed a significant (** $p < 0.01$, *** $p < 0.001$, $n = 6$; one way ANOVA with Dunnett's posthoc test) reduction in total cholesterol, TGs, and LDL cholesterol as compared to diabetic control mice. The high-density lipoprotein (HDL) cholesterol level in diabetic control mice was significantly decreased ($p < 0.05$, $n = 6$; Student's t test) as compared to normal control. The effect on HDL level was comparable with the glibenclamide (0.5 mg/kg) treated mice. Myrrhanol-B, and Myrrhanone-B treated groups and standard glibenclamide significantly (** $p < 0.01$, *** $p < 0.001$, $n = 6$; one way ANOVA with Dunnett's posthoc test) increased the HDL cholesterol level in diabetic mice.

3.6. Effect of myrrhanol-B, myrrhanone-B serum profile in alloxan-induced diabetic mice

The effects of alloxan on the activity of hepatic marker enzymes in serum are given in Table 4. In the present study, the levels of serum glutamate pyruvate transaminase (SGPT), serum glutamate oxaloacetate transaminase (SGOT) and alkaline phosphatase (ALP) in alloxan-induced diabetic mice were elevated. The administration of Myrrhanol-B, and Myrrhanone-B in 5 at 10 mg/kg for 21 days showed a significant (** $p < 0.01$, *** $p < 0.001$ $n = 6$; one way ANOVA with Dunnett's posthoc test) reduction in serum SGPT, SGOT, ALP and creatinine in mice intoxicated with alloxan, these results are comparable to standard drug glibenclamide.

3.7. In-silico target prediction by Molecular Docking

α-Glucosidase enzyme serves as the prominent drug target to control hyperglycemic effects in diabetes [50], therefore, α-glucosidase was

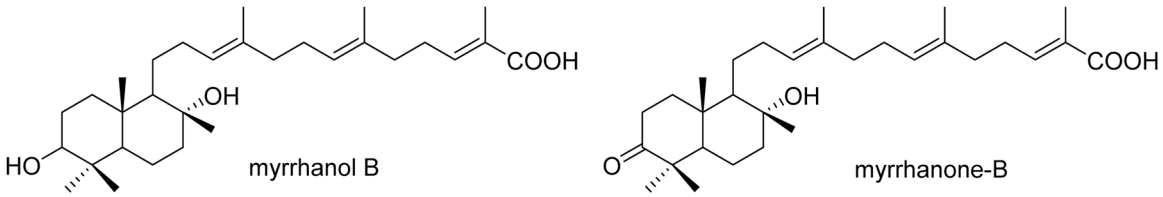

Fig. 1. Structures of the Myrrhanone-B and Myrrhanol-B.

Table 1
The effect of daily Intraperitoneal administration of ml, MN, and Glibenclamide on blood glucose level of Alloxan-induced diabetic mice.

S. No.	Groups	Dose mg/kg	Day[1st]	Day[4th]	Day[7th]	Day[10th]	Day[15th]	Day[21st]
1	Normal control	0.4 ml	90 ± 2	93.2 ± 4	101 ± 6	92 ± 2	95 ± 4	98 ± 4
2	Diabetic control	0.4 ml	268.2 ± 11	295 ± 15	310 ± 26	316 ± 25	322 ± 23	337 ± 27
3	Glibenclamide	0.5	257.6 ± 14	223.7 ± 4 *	205 ± 18 **	180 ± 22 **	142 ± 12 ***	130 ± 16 ***
4	Myrrhanol-B	5	249.5 ± 10	228.4 ± 8 *	215 ± 14 *	208 ± 17 *	187 ± 11 **	168 ± 32 **
5	Myrrhanol-B	10	265.2 ± 11	242.4 ± 8 *	217 ± 12 **	188 ± 13 **	164 ± 18 **	141 ± 22 ***
6	Myrrhanone-B	5	260.3 ± 14	240.6 ± 32 *	218 ± 18 *	203 ± 34 *	190 ± 24 **	175 ± 24 **
7	Myrrhanone-B	10	253.8 ± 25	237 ± 10 *	209 ± 24 *	191 ± 10 **	183 ± 10 **	165 ± 10 ***

The values are expressed as mean ± SEM. (n = 6 in each group). *P< 0.05, * *P< 0.01, * **P< 0.001 as compared with diabetic control at the same time (one-way ANOVA followed by Dunnett's multiple comparison test).

Table 2
The effects of Myrrhanol-B, Myrrhanone-B on percentage bodyweight (B.W) in alloxan-induced diabetic mice.

Groups	Dose mg/kg	Day 1st	Day 4th	Day 7th	Day 10th	Day 15th	Day 21st	% Change in body weight
[a]Normal control	0.4 ml	20 ± 0.4	22 ± 3	24.5 ± 2	26 ± 1	27.5 ± 2	28 ± 2	
[b]Diabetic control	0.4 ml	23 ± 2	24 ± 3 *	20 ± 2 *	18.5 ± 1 * *	16 ± 2 **	14.5 ± 2 ***	-11.5
[c]Glibenclamide	0.5	21 ± 4	23 ± 2 *	25 ± 1 *	27 ± 2 * *	28.5 ± 2 **	31 ± 1 ***	± 9.33
[c]Myrrhanol-B	5	23 ± 3	24.5 ± 2 *	25.5 ± 3 *	26.5 ± 1 *	27 ± 2 *	27.5 ± 2 *	± 4.2
[c]Myrrhanol-B	10	21 ± 2	23 ± 4 *	24.5 ± 1 *	26 ± 2 * *	27.5 ± 2 **	29.5 ± 2 **	± 8.2
[c]Myrrhanone-B	5	23 ± 2	24 ± 1 *	24.5 ± 2 *	26 ± 2 *	26.5 ± 2 *	27 ± 2 *	± 3.5
[c]Myrrhanone-B	10	22 ± 1	24 ± 2 *	25.5 ± 1 *	27.5 ± 2 *	28 ± 1 **	28.5 ± 2 **	± 6.16

The values are expressed as mean ± SEM. Each value corresponds to a mean of six animals. * $P < 0.05$, ** $p < 0.01$, *** $p < 0.001$; comparison of [a](normal control) *vs* [b](diabetic control) (Student t-test), *$P < 0.05$, * *$p < 0.01$; comparison of [b] (diabetic control) *vs* [c] (Glibenclamide and compounds treated groups) (one way ANOVA followed by Dunnett's posthoc multiple comparison test). %Change in BW : $\frac{\text{Initial weigh(g)} - \text{Finial weight(g)}}{\text{Initial weigh(g)}} \times 100$

Table 3
The effects of myrrhanol-B and myrrhanone-B on lipid profile in alloxan-induced diabetic mice.

S.NO	Groups	Dose mg/kg	Total cholesterol (mg/dl)	TG (mg/dl)	HDL (mg/dl)	LDL (mg/dl)
1	[a]Normal control	0.4 ml	132 ± 4.14	130.2 ± 1.1	23.4 ± 0.8	88 ± 2.6
2	[b]Diabetic control	0.4 ml	268 ± 2.3 **	312.4 ± 1.05 **	19.6 ± 2.1 *	155.6 ± 2.8 **
3	[c]Glibenclamide	0.5	141.8 ± 4.6 **	125.5 ± 2.2 **	37.2 ± 1.4 **	67.8 ± 2.2 ***
4	[c]Myrrhanol-B	5	155 ± 4.1 **	133.6 ± 5.5 **	27.2 ± 1.1 **	86.2 ± 2.0 **
5	[c]Myrrhanol-B	10	144 ± 3.3 **	130.4 ± 5.5 **	34.6 ± 5.5 **	74.2 ± 3.0 ***
6	[c]Myrrhanone-B	5	165.2 ± 3.1 *	144.2 ± 2.1 *	25.5 ± 2.1 *	92.8 ± 4.0 **
7	[c]Myrrhanone-B	10	159 ± 2.4 *	136.4 ± 2.2 **	31.6 ± 2.4 **	79.1 ± 3.5 **

Each value is mean ± SEM of eight animals. Comparisons were made between [a]normal control and [b]Diabetic control using Student t-test (*$p < 0.05$, **$p < 0.01$) and between [b]Diabetic control and [c](Glibenclamide/compounds) treated groups using one way ANOVA followed by Dunnett's posthoc multiple comparison test (*$p < 0.05$, **$p < 0.01$, ***$p < 0.001$).

Table 4
The effects of myrrhanol-B, and myrrhanone-B on serum profile in alloxan-induced diabetic mice.

S.NO	Groups	Dose mg/kg	(SGPT)IU	(SGOT)IU	(ALP)IU	Serum creatinine (mg/dl)
1	[a]Normal control	0.4 ml	22 ± 2.2	19 ± 8.5	130 ± 2.2	0.4 ± 0.4
2	[b]Diabetic control	0.4 ml	68 ± 5.5	44 ± 2.8 **	278 ± 1.1 **	3.4 ± 0.2 **
3	[c]Glibenclamide	0.5	25 ± 2.6 **	23 ± 5.1 **	136 ± 3.1 **	0.5 ± 0.4 ***
4	[c]Myrrhanol-B	5	34 ± 4.1 **	26 ± 2.2 **	149 ± 4.4 **	0.6 ± 0.2 **
5	[c]Myrrhanol-B	10	27 ± 6.3 **	24 ± 6.5 **	139 ± 4.1 **	0.5 ± 0.1 ***
6	[c]Myrrhanone-B	5	37 ± 2.2 *	29 ± 4.1 **	165 ± 10.2 **	0.6 ± 0.3 **
7	[c]Myrrhanone-B	10	31 ± 4.1 **	27 ± 4.1 **	152 ± 2.4 **	0.7 ± 0.1 **

Each value is mean ± SEM of eight animals. Comparisons were made between [a]normal control and [b]Diabetic control using Student t-test (*$p < 0.05$, **$p < 0.01$) and between [b]Diabetic control and [c](Glibenclamide/compounds) treated groups using one way ANOVA followed by Dunnett's posthoc multiple comparison test (*$p < 0.05$, **$p < 0.01$, ***$p < 0.001$).

selected as a molecular target of our compounds for molecular docking studies. The structure of α-glucosidase was taken from AlphaFold server with a high confidence score (>90%) for 97% of residues (Fig. 2A). Before refining the homology model, a Ramachandran plot revealed that 81.8%, 17.4%, and 0.6% of the residues resides in favored, additionally allowed, and generously allowed regions, respectively, while only 0.2% of residues are in the disallowed region (Fig. 2C). The homology model was then refined through simulation, and its stability was assessed by root mean square deviation (RMSD) over a simulation time of 1 μs. Initially, the RMSD was increased to ~2.8 Å during the first 100 ns but reached equilibrium by the end of the simulation, with an average RMSD of 2.92 Å (Fig. 2E). The root means square fluctuation (RMSF) analysis indicates high flexibility in four loop regions (L1-L4) and one alpha helix (H1), with L1 showing the most significant fluctuation of 6 Å due to loop conformation. The radius of gyration (Rg) analysis demonstrates that the α-glucosidase structure maintains high compactness throughout the

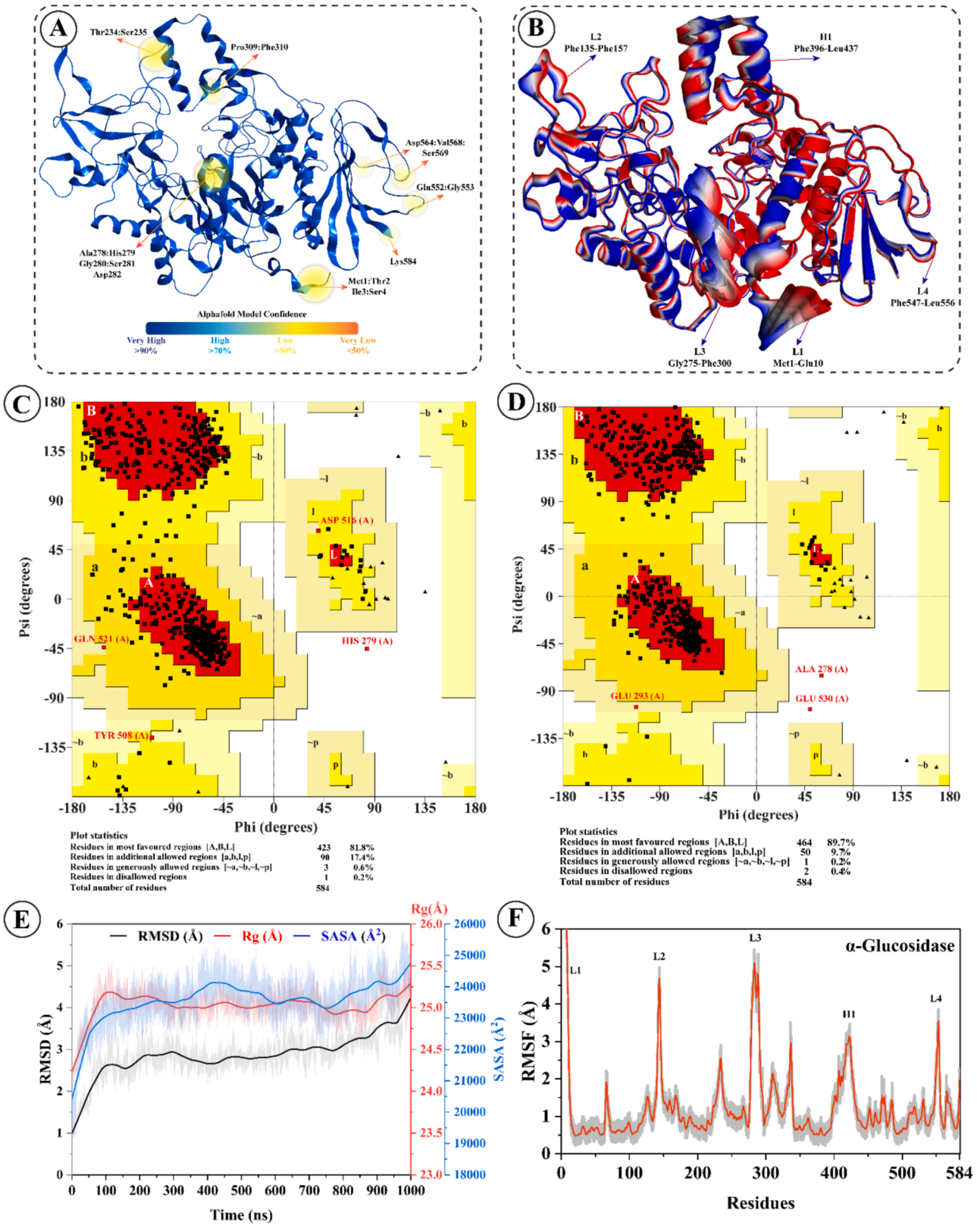

Fig. 2. . (A) The α-glucosidase model retrieved from the Alpha Fold server (code P38158). **(B)** The conformational changes in α-glucosidase structure are shown during the simulation, represented by a color gradient from blue-to-red. **(C)** and **(D)** show the Ramachandran plot before and after simulation, respectively. **(E)** The analysis of the RMSD, Rg, and SASA of the homology model during the simulation. **(F)** The fluctuation of residues of α-glucosidase during the simulation, as observed by RMSF analysis.

simulation, with an average Rg value of 25.02 Å. The solvent accessible surface area (SASA) analysis showed an initial increase in the overall SASA to an average of 23000 $Å^2$ during the first 100 ns, followed by stabilization at an average of 23571 $Å^2$ until the end of the simulation. The structural dynamics of the protein throughout the simulation is illustrated in Fig. 2B, with colors representing the start (blue) and end (red) states. After the simulation, a Ramachandran plot shows 89.7% residues in the favored region, while additional allowed, generously allowed, and disallowed regions accounted for 9.7%, 0.2%, and 0.04% of the residues, respectively (Fig. 2D). This suggests an improvement in the overall protein structure following the molecular dynamics (MD) simulation.

During docking, we observed that the residues Asp214, Glu276, and Asp349 within the active pocket of α-glucosidase are responsible for its catalytic function. Specifically, Asp214 and Asp349 form multiple hydrogen bonds with the compounds selected in this study (Fig. 3). The most active compound, Myrrhanol-B, interacts with key residues including Asp214, Asp349, Asn347, Arg439, Arg443, and Tyr23, all of which are part of the active site. Furthermore, Arg439 and Arg443 form ionic bonds with the Myrrhanol-B. Another promising compound, Myrrhanone-B, forms strong hydrogen bonds with side chain of Asp214, Arg312, Ile109, and Asn110, which are also part of the catalytic residues. These interactions demonstrate that both the compounds have strong affinity for the catalytic triad residues and fit well in the α-glucosidase active pocket. The atom-based interactions and docking scores of each compound is given in Table 5.

3.8. *In-vitro evaluation of α-Glucosidase inhibitory potential and Kinetic studies*

The binding affinities predicted by molecular docking were further confirmed by *in-vitro* testing of Myrrhanone-B and Myrrhanol-B against α-glucosidase. Fortunately, both compounds exhibited potent inhibition of α-glucosidase with IC_{50} values of 19.50 ± 0.71, and 16.11 ± 0.69 μM, respectively. The mechanism of action of both compounds was studied to reveal their binding affinity with the active site residues. In the kinetics studies, Myrrhanol-B displayed a mixed type of inhibition with *Ki* value of 12.33 ± 0.030 μM. In mixed type of inhibition, the inhibitor binds with active site residue as well as other than active site residues and this pattern of inhibition decrease *Vmax* of the enzyme while *Km* value increases (Fig. 4). While Myrrhanone-B exhibits competitive type of inhibition with *Ki* value of 14.53 ± 0.040 μM. In such type of

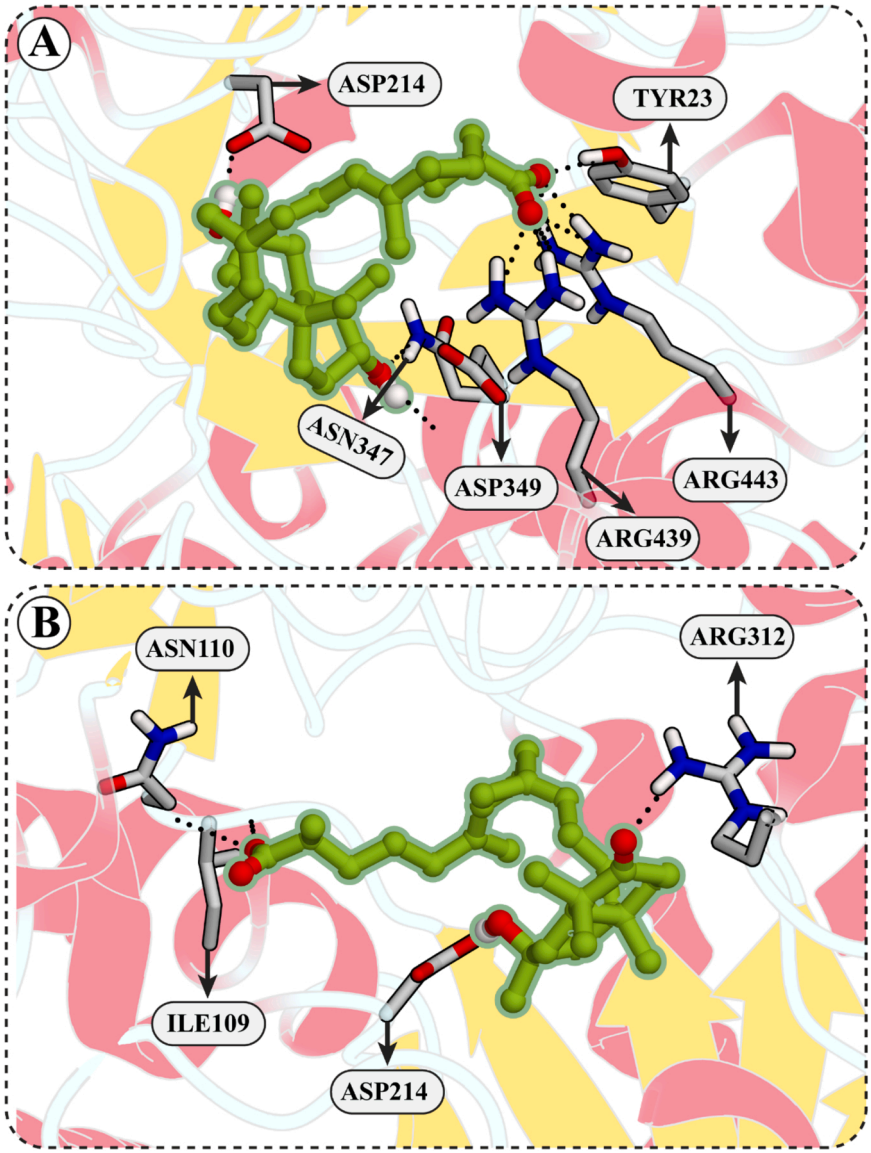

Fig. 3. The interactions between the (A) Myrrhanol-B and (B) Myrrhanone-B, with the active site residues of α-glucosidase are shown.

Table 5
The interactions between myrrhanol-B, and myrrhanone-B with the active site residues of α-glucosidase.

Compounds	Ligand Atoms	Receptor Atoms	Residues	Bond Type	Distance (Å)	Energy (kcal/mol)
Myrrhanol-B	O30	OD1	ASP214	HBD	2.68	-3.1
	O31	O	ASP349	HBD	2.69	-0.9
	O31	ND2	ASN347	HBA	2.93	-2.7
	O33	NH1	ARG439	HBA	2.72	-12.8
	O33	NH2	ARG439	HBA	2.76	-3.5
	O33	NH1	ARG443	HBA	2.73	-7.4
	O34	OH	TYR23	HBA	2.64	-3.8
	O34	NH1	ARG443	HBA	2.85	-5.6
	O34	NH2	ARG443	HBA	2.71	-4.9
	O33	NH1	ARG439	Ionic	2.72	-6.6
	O33	NH2	ARG439	Ionic	2.76	-6.3
	O33	NH1	ARG443	Ionic	2.73	-6.6
	O33	NH2	ARG443	Ionic	3.41	-2.2
	O34	NH1	ARG443	Ionic	2.85	-5.6
	O34	NH2	ARG443	Ionic	2.71	-6.7
Myrrhanone-B	O31	OD2	ASP214	HBD	2.77	-3.1
	O11	NH1	ARG312	HBA	2.8	-4.6
	O34	N	ILE109	HBA	2.74	-8.8
	O34	N	ASN110	HBA	2.8	-5.4

HBA = hydrogen bond acceptor, HBD = hydrogen bond donor

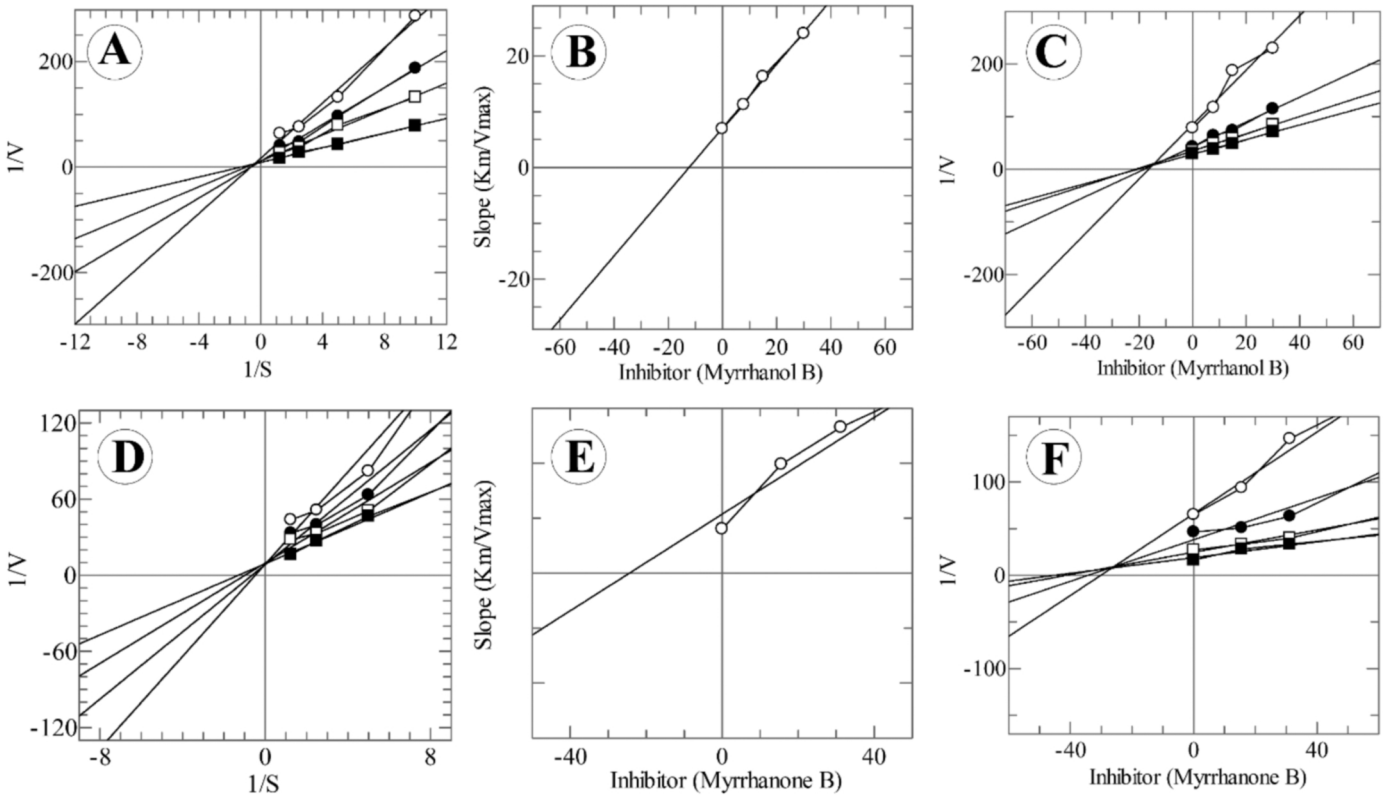

Fig. 4. Mode of inhibition of α-glucosidase by **Myrrhanol-B**, and **Myrrhanone-B** (A, D) Line weaver-Burk plot of reciprocal of rate of reaction (velocities) *vs* reciprocal of substrate (4-nitro phenyl-α-D-glucopyranoside) in the absence of **Myrrhanol-B**, and **Myrrhanone-B** (■), and in the presence of **Myrrhanol-B**, and **Myrrhanone-B** at 30.00 μ*M* (○), 15.00 μ*M* (●), and 7.8125 μ*M* (□) respectively. Secondary replot of Line weaver-Burk plot between the slopes of each line on-Line weaver-Burk plot *vs* different concentrations of **Myrrhanol-B**, and **Myrrhanone-B** (B, E). Dixon plot of reciprocal of rate of reaction (velocities) *vs* different concentrations of **Myrrhanol-B**, and **Myrrhanone-B** (C, F).

inhibition, Km value increases, while Vmax remains constant (Fig. 4).

4. Discussion

Despite the availability of proven antidiabetic drugs, the ethnobotanical community is quite interested in natural chemicals derived from plants and preparations because of their less harmfulness and side effects than the synthetic agents [51,52]. Alloxan [2,4,5,6-tetraoxypyrimidine; 5,6-dioxyuracil] is a pyrimidine derivative of uric acid, initially discovered by Brugnaletti in 1818 and later by Wohler in 1838. This compound revealed diabetogenic effects in 1943 when central islet necrosis was found in alloxan-treated rabbits. Since then, it has been used to model Type 1 diabetes in animal experimentation. Doses varies in different studies; however, it is suggested that single doses ranging from 50 to 150 mg/kg produce chronic hyperglycemia in rodents depending on administration route and strain [53].

The current study shows that the compounds Myrrhanone-B and Myrrhanol-B considerably lowered the blood glucose levels in mice in which diabetes is induced by alloxan (120 mg/kg). Moreover, Myrrhanone-B and Myrrhanol-B also showed antihyperglycemic properties because they limit the formation of free radicals, which are produced when alloxan is administered intraperitoneally to mice. Increase in total cholesterol, triglycerides, and low-density lipoprotein (which are key contributors to cardiovascular illnesses) was observed in the diabetic control group. The lipid profile in diabetic mice is reduced after the administration of Myrrhanol-B and Myrrhanone-B at doses of 5 and 10 mg/kg, respectively. Additionally, the diabetic control group consistently lost body weight, which was reversed in the Myrrhanol-B and Myrrhanone-B treated groups. Furthermore, significant improvement in body weight was seen in the groups receiving the treatment. According to reports, alloxan-induced diabetic mice liver cells are irreversibly annihilated leading the hepatic microsomal cells to discharge a variety of enzymes into the bloodstream including SGPT, SGOT, and serum ALP, thereby increases the plasma levels of these enzymes [54]. In our observation, the levels of SGPT, SGOT, and ALP were substantially decreased by Myrrhanol-B and Myrrhanone-B. Renal dysfunction is caused by chronic hyperglycemia, which raises serum creatinine and uric acid levels [55,56]. We also observed that Myrrhanol-B and Myrrhanone-B can lower serum creatinine levels in alloxan-induced diabetic mice, thus, aids the treatment and protects the renal system. These results support the idea that these natural compounds can have a significant role in protecting the vital organs (kidney, liver, and pancreas), which lowers the incidence of diabetes in test animals.

Computational procedures are widely used in the prediction and identification of drugs targets for several diseases [50,57]. Herein, α-glucosidase enzyme was selected as target for Myrrhanol-B and Myrrhanone-B and their binding affinities were estimated through computational docking. Inhibiting α-glucosidase has emerged as a successful strategy for the treatment of type 2 DM to reduce high blood glucose levels. The final step in the digestion of carbohydrates before they are absorbed into the blood from the small intestine is catalyzed by this hydrolase enzyme, which is why α-glucosidase inhibitors (AGIs) slow down this process. [58]. The predicted target α-glucosidase was further confirmed by *in-vitro* testing of Myrrhanone-B and Myrrhanol-B against α-glucosidase. Interestingly, both compounds showed significant inhibition of α-glucosidase with IC_{50} values of 19.50 ± 0.71 μM and 16.11 ± 0.69 μM, respectively as compared to standard drug acarbose. The kinetics studies were used to reveal the mechanism of action of Myrrhanone-B and Myrrhanol-B against α-glucosidase which revealed that Myrrhanol-B and Myrrhanone-B has a mixed and competitive type of inhibition with *Ki* value of 12.33 ± 0.030 μM and 14.53 ± 0.040 μM, respectively.

5. Conclusion

In order to search novel anti-diabetic compounds, two natural products, namely Myrrhanone-B and Myrrhanol-B (isolated from *Commiphora mukul* Hook) were evaluated *in-vivo*. In the *in-vivo* studies, these molecules demonstrated significant anti-diabetic and anti-hyperlipidemic effects. Furthermore, these molecules improved the abnormal level of total cholesterol, triacylglycerol (TG), and low-density lipoprotein cholesterol (LDL-C) to a normal level and increased the level of high-density lipoprotein cholesterol. Their mode of inhibition was predicted by *in-silico* molecular docking approach which suggests that these molecules inhibit the function of α-glucosidase enzyme by binding with its active site residues through highly negative docking scores. The *in-silico* predicted target was further confirmed by *in-vitro* α-glucosidase enzyme inhibition assay in which both the compounds displayed excellent α-glucosidase inhibition in < 20 μM. We further examined the mechanism of inhibition of these inhibitors by kinetic experiments, where Myrrhanol-B and Myrrhanone-B has shown mixed and competitive type of inhibition, respectively.

Ethics approval and consent to participate

The experimental procedures on animals were approved by the Institutional Ethical Committee of (DAEC/PHARM/2016/15) of University of Swabi, KPK, Pakistan and were carried out in compliance with the 1986 UK Animal Scientific Procedure Act.

Funding

The authors would like to extend their gratitude to King Saud University (Riyadh, Saudi Arabia) for funding this research through Researchers supporting Project number (RSP-2023-R406). The project was supported by grant from The Oman Research Council (TRC) through the funded project (BFP/RGP/CBS/21/002).

CRediT authorship contribution statement

AK and AAH conceived and designed the study. WUI and FK performed *in-vivo* experiments. NUR performed isolation. MW and SAH performed computational analysis and SU performed *in-vitro* testing. HK, MHM and GEB analyzed the data. WUI, MW and FK wrote the manuscript with input, SAH proofread the manuscript and comments from all co-authors. All authors have read and approved the final version of the manuscript.

Declaration of Competing Interest

The authors declare that they have no known competing financial interests or personal relationships that could have appeared to influence the work reported in this paper.

Data Availability

Anything related to this article, can be obtained from the corresponding authors.

Acknowledgments

The authors would like to extend their gratitude to King Saud University (Riyadh, Saudi Arabia) for funding this research through Researchers supporting Project number (RSP-2023-R406).

Consent for Publication

Not relevant.

References

[1] E.W. Yue, B. Wayland, B. Douty, M.L. Crawley, E. McLaughlin, A. Takvorian, Z. Wasserman, M.J. Bower, M. Wei, Y. Li, Isothiazolidinone heterocycles as inhibitors of protein tyrosine phosphatases: synthesis and structure–activity relationships of a peptide scaffold, Bioorg. Med. Chem. 14 (17) (2006) 5833–5849.
[2] Y. Zhu, Y. Zhang, Y. Liu, H. Chu, H. Duan, Synthesis and biological activity of transtiliroside derivatives as potent anti-diabetic agents, Molecules 15 (12) (2010) 9174–9183.
[3] A.D. McInnes, Diabetic foot disease in the United Kingdom: about time to put feet first, J. Foot ankle Res. 5 (1) (2012) 1–7.
[4] M. Cardenas, J. Miranda, D. Beran, Delivery of Type 2 diabetes care in low-and middle-income countries: lessons from Lima, Peru, Diabet. Med. 33 (6) (2016) 752–760.
[5] E. Adeghate, P. Schattner, E. Dunn, An update on the etiology and epidemiology of diabetes mellitus, Ann. N. Y. Acad. Sci. 1084 (1) (2006) 1–29.
[6] P. Saeedi, I. Petersohn, P. Salpea, B. Malanda, S. Karuranga, N. Unwin, S. Colagiuri, L. Guariguata, A.A. Motala, K. Ogurtsova, Global and regional diabetes prevalence estimates for 2019 and projections for 2030 and 2045: results from the international diabetes federation diabetes atlas, Diabetes Res. Clin. Pract. 157 (2019), 107843.
[7] B. Fletcher, M. Gulanick, C. Lamendola, Risk factors for type 2 diabetes mellitus, J. Cardiovasc. Nurs. 16 (2) (2002) 17–23.
[8] K.G.M.M. Alberti, P. Zimmet, J. Shaw, International diabetes federation: a consensus on type 2 diabetes prevention, Diabet. Med. 24 (5) (2007) 451–463.

[9] Z.A. Bhutta, R.A. Salam, A. Gomber, L. Lewis-Watts, T. Narang, J.C. Mbanya, G. Alleyne, A century past the discovery of insulin: global progress and challenges for type 1 diabetes among children and adolescents in low-income and middle-income countries, Lancet 398 (10313) (2021) 1837–1850.

[10] B.B. Zhang, D.E. Moller, New approaches in the treatment of type 2 diabetes, Curr. Opin. Chem. Biol. 4 (4) (2000) 461–467.

[11] K. Ansari, C. Lal, Synthesis and biological activity of some heterocyclic compounds containing benzimidazole and beta-lactam moiety, J. Chem. Sci. 121 (2009) 1017–1025.

[12] M.A.M. Maciel, A.C. Pinto, V.F. Veiga Jr, N.F. Grynberg, A. Echevarria, Medicinal plants: the need for multidisciplinary scientific studies, Quím. Nova 25 (2002) 429–438.

[13] N.U. Rehman, A. Khan, A. Al-Harrasi, H. Hussain, A. Wadood, M. Riaz, Z. Al-Abri, New α-glucosidase inhibitors from the resins of Boswellia species with structure–glucosidase activity and molecular docking studies, Bioorg. Chem. 79 (2018) 27–33.

[14] G. Janssen, U. Bode, H. Breu, B. Dohrn, V. Engelbrecht, U. Göbel, Boswellic acids in the palliative therapy of children with progressive or relapsed brain tumors, Klin. Pädiatrie 212 (04) (2000) 189–195.

[15] B.K. Rao, R. Giri, M. Kesavulu, C. Apparao, Effect of oral administration of bark extracts of Pterocarpus santalinus L. on blood glucose level in experimental animals, J. Ethnopharmacol. 74 (1) (2001) 69–74.

[16] G. Mariappan, B. Saha, S. Datta, D. Kumar, P. Haldar, Design, synthesis and antidiabetic evaluation of oxazolone derivatives, J. Chem. Sci. 123 (2011) 335–341.

[17] N.U. Rehman, H. Hussain, H.Y. Khan, R. Csuk, G. Abbas, I.R. Green, A. Al-Harrasi, A norterpenoid and tripenoids from *Commiphora mukul*: isolation and biological activity, Z. für Naturforsch. B 72 (1) (2017) 11–15.

[18] B. Mesrob, C. Nesbitt, R. Misra, R.C. Pandey, High-performance liquid chromatographic method for fingerprinting and quantitative determination of E- and Z-guggulsterones in *Commiphora mukul* resin and its products, J. Chromatogr. B 720 (1–2) (1998) 189–196.

[19] H. Matsuda, T. Morikawa, S. Ando, H. Oominami, T. Murakami, I. Kimura, M. Yoshikawa, Absolute stereostructures of polypodane-and octanordammarane-type triterpenes with nitric oxide production inhibitory activity from guggul-gum resins, Bioorg. Med. Chem. 12 (11) (2004) 3037–3046.

[20] U.V. Mallavadhani, M. Chandrashekhar, K. Shailaja, S. Ramakrishna, Design, synthesis, anti-inflammatory, cytotoxic and cell based studies of some novel side chain analogues of myrrhanones A & B isolated from the gum resin of *Commiphora mukul*, Bioorg. Chem. 82 (2019) 306–323.

[21] B.B. Singh, L.C. Mishra, S.P. Vinjamury, N. Aquilina, V. Singh, N. Shepard, The effectiveness of *Commiphora mukul* for osteoarthritis of the knee: an outcomes study, Altern. Ther. Health Med. 9 (3) (2003) 74–81.

[22] K. Singh, R. Chander, N.K. Kapoor, Guggulsterone, a potent hypolipidaemic, prevents oxidation of low density lipoprotein, Phytotherapy Research, Int. J. Devoted Med. Sci. Res. Plants Plant Prod. 11 (4) (1997) 291–294.

[23] V. Singh, S. Kaul, R. Chander, N. Kapoor, Stimulation of low density lipoprotein receptor activity in liver membrane of guggulsterone treated rats, Pharmacol. Res. 22 (1) (1990) 37–44.

[24] A.-S. Abdul-Ghani, R. Amin, Effect of aqueous extract of *Commiphora opobalsamum* on blood pressure and heart rate in rats, J. Ethnopharmacol. 57 (3) (1997) 219–222.

[25] T. Al-Howiriny, M. Al-Sohaibani, M. Al-Said, M. Al-Yahya, K. El-Tahir, S. Rafatullah, Effect of Commiphora opobalsamum (L.) Engl.(Balessan) on experimental gastric ulcers and secretion in rats, J. Ethnopharmacol. 98 (3) (2005) 287–294.

[26] T. Al-Howiriny, M. Al-Sohaibani, M. Al-Said, M. Al-Yahya, K. El-Tahir, S. Rafatullah, Hepatoprotective properties of *Commiphora opobalsamum* (" Balessan"), a traditional medicinal plant of Saudi Arabia, Drugs Exp. Clin. Res. 30 (5–6) (2004) 213–220.

[27] L.O. Hanuš, T. Řezanka, V.M. Dembitsky, A. Moussaieff, Myrrh-commiphora chemistry, Biomed. Pap. 149 (1) (2005) 3–28.

[28] I. Kimura, M. Yoshikawa, S. Kobayashi, Y. Sugihara, M. Suzuki, H. Oominami, T. Murakami, H. Matsuda, V.V. Doiphode, New triterpenes, myrrhanol A and myrrhanone A, from guggul-gum resins, and their potent anti-inflammatory effect on adjuvant-induced air-pouch granuloma of mice, Bioorg. Med. Chem. Lett. 11 (8) (2001) 985–989.

[29] A. Khan, R. Gul, N.U. Rehman, H. Khan, N. Karim, S.A. Halim, S. Ahmed, A. Al-Harrasi, Myrrhanone B and Myrrhanol B from resin of *Commipohora mukul* exhibit hepatoprotective effects in-vivo, Biomed. Pharmacother. 143 (2021), 112131.

[30] S. Irvin, comprehensive observational assessment: a systematic quantitative procedure for assess_ing the behavioral and physiologic state of the mouse, Phychopharmacologia 13 (3) (1968) 222–257.

[31] Y.M. Belayneh, E.M. Birru, Antidiabetic activities of hydromethanolic leaf extract of *Calpurnia aurea* (Ait.) Benth. Subspecies aurea (Fabaceae) in mice, Evid. Based Complement. Altern. Med. (2018) (2018).

[32] M. Sefi, H. Fetoui, M. Makni, N. Zeghal, Mitigating effects of antioxidant properties of *Artemisia campestris* leaf extract on hyperlipidemia, advanced glycation end products and oxidative stress in alloxan-induced diabetic rats, Food Chem. Toxicol. 48 (7) (2010) 1986–1993.

[33] A. Nagappa, P. Thakurdesai, N.V. Rao, J. Singh, Antidiabetic activity of Terminalia catappa Linn fruits, J. Ethnopharmacol. 88 (1) (2003) 45–50.

[34] I. Khan, W. Ahmad, N. Karim, M. Ahmad, M. Khan, S.A. Tariq, N. Sultana, R. Shah, A. Khan, A. Abdelhalim, Antidiabetic activity and histopathological analysis of carnosol isolated from *Artemisia indica* linn in streptozotocin-induced diabetic rats, Med. Chem. Res. 26 (2017) 335–343.

[35] C.C.G. ULC, Molecular Operating Environment (MOE), 2020.09, 1010 Sherbrooke St. West, Suite #910, Montreal, QC, Canada, H3A 2R7, 2020.

[36] P.R. Gerber, K. Müller, MAB, a generally applicable molecular force field for structure modelling in medicinal chemistry, J. Comput. -Aided Mol. Des. 9 (3) (1995) 251–268.

[37] J.A. Maier, C. Martinez, K. Kasavajhala, L. Wickstrom, K.E. Hauser, C. Simmerling, ff14SB: improving the accuracy of protein side chain and backbone parameters from ff99SB, J. Chem. Theory Comput. 11 (8) (2015) 3696–3713.

[38] C. Tian, K. Kasavajhala, K.A. Belfon, L. Raguette, H. Huang, A.N. Migues, J. Bickel, Y. Wang, J. Pincay, Q. Wu, ff19SB: Amino-acid-specific protein backbone parameters trained against quantum mechanics energy surfaces in solution, J. Chem. Theory Comput. 16 (1) (2019) 528–552.

[39] R. Salomon-Ferrer, A.W. Gotz, D. Poole, S. Le Grand, R.C. Walker, Routine microsecond molecular dynamics simulations with AMBER on GPUs. 2. Explicit solvent particle mesh Ewald, J. Chem. Theory Comput. 9 (9) (2013) 3878–3888.

[40] W.H. Press, B.P. Flannery, S.A. Teukolsky, W.T. Vetterling, P.B. Kramer, Numerical recipes: the art of scientific computing, Phys. Today 40 (10) (1987) 120.

[41] D.J. Sindhikara, S. Kim, A.F. Voter, A.E. Roitberg, Bad seeds sprout perilous dynamics: stochastic thermostat induced trajectory synchronization in biomolecules, J. Chem. Theory Comput. 5 (6) (2009) 1624–1631.

[42] V. Kräutler, W.F. Van Gunsteren, P.H. Hünenberger, A fast SHAKE algorithm to solve distance constraint equations for small molecules in molecular dynamics simulations, J. Comput. Chem. 22 (5) (2001) 501–508.

[43] D.R. Roe, T.E. Cheatham III, PTRAJ and CPPTRAJ: software for processing and analysis of molecular dynamics trajectory data, J. Chem. Theory Comput. 9 (7) (2013) 3084–3095.

[44] R.A. Laskowski, M.W. MacArthur, D.S. Moss, J.M. Thornton, PROCHECK: a program to check the stereochemical quality of protein structures, J. Appl. Crystallogr. 26 (2) (1993) 283–291.

[45] R.A. Laskowski, PDBsum: summaries and analyses of PDB structures, Nucleic Acids Res. 29 (1) (2001) 221–222.

[46] C.C.G. ULC, Molecular Operating Environment (MOE), 2022.02, 1010 Sherbrooke St. West, Suite #910, Montreal, QC, Canada, H3A 2R7, 2022.

[47] M. Shah, H. Rahman, A. Khan, S. Bibi, O. Ullah, S. Ullah, N. Ur Rehman, W. Murad, A. Al-Harrasi, Identification of α-glucosidase inhibitors from Scutellaria edelbergii: ESI-LC-MS and computational approach, Molecules 27 (4) (2022) 1322.

[48] N. Kausar, S. Ullah, M.A. Khan, H. Zafar, M.I. Choudhary, S. Yousuf, Celebrex derivatives: Synthesis, α-glucosidase inhibition, crystal structures and molecular docking studies, Bioorg. Chem. 106 (2021), 104499.

[49] N.C. Chaulya, P.K. Haldar, A. Mukherjee, Antidiabetic activity of methanol extract of rhizomes of Cyperus tegetum Roxb.(Cyperaceae), Acta Pol. Pharm. 68 (6) (2011) 989–992.

[50] S.A. Halim, S. Jabeen, A. Khan, A. Al-Harrasi, Rational design of novel inhibitors of α-glucosidase: an application of quantitative structure activity relationship and structure-based virtual screening, Pharmaceuticals 14 (5) (2021) 482.

[51] K. Anand, C. Tiloke, P. Naidoo, A. Chuturgoon, Phytonanotherapy for management of diabetes using green synthesis nanoparticles, J. Photochem. Photobiol. B: Biol. 173 (2017) 626–639.

[52] M.J. Balick, P.A. Cox, Plants, People, and Culture: the Science of Ethnobotany, Garland Science, 2020.

[53] A. King, Animal Models of Type 1 and Type 2 Diabetes Mellitus, Animal Models for the Study of Human Disease, Elsevier, 2017, pp. 245–265.

[54] T.S. Dhas, V.G. Kumar, V. Karthick, K. Vasanth, G. Singaravelu, K. Govindaraju, Effect of biosynthesized gold nanoparticles by Sargassum swartzii in alloxan induced diabetic rats, Enzym. Microb. Technol. 95 (2016) 100–106.

[55] N. Amartey, K. Nsiah, F. Mensah, Plasma levels of uric acid, urea and creatinine in diabetics who visit the clinical analysis laboratory (CAn-Lab) at Kwame Nkrumah University of Science and Technology, Kumasi, Ghana, J. Clin. Diagn. Res.: JCDR 9 (2) (2015) BC05.

[56] O.H. Azeez, S.Y. Alkass, D.S. Persike, Long-term saccharin consumption and increased risk of obesity, diabetes, hepatic dysfunction, and renal impairment in rats, Medicina 55 (10) (2019) 681.

[57] A. Khan, I. Khan, S.A. Halim, N.U. Rehman, N. Karim, W. Ahmad, M. Khan, R. Csuk, A. Al-Harrasi, Anti-diabetic potential of β-boswellic acid and 11-keto-β-boswellic acid: mechanistic insights from computational and biochemical approaches, Biomed. Pharmacother. 147 (2022), 112669.

[58] S. Wali, S. Ullah, M.A. Khan, S. Hussain, M. Shaikh, M.I. Choudhary, Synthesis of new clioquinol derivatives as potent α-glucosidase inhibitors; molecular docking, kinetic and structure–activity relationship studies, Bioorg. Chem. 119 (2022), 105506.